TC-1893

SENSIBLE AND LATENT HEAT BUFFER STORAGE RECEIVER SYSTEMS FOR DISH MOUNTED SOLAR APPLICATION

Hanford Engineering Development Laboratory

HANFORD ENGINEERING DEVELOPMENT LABORATORY
Operated by Westinghouse Hanford Company
P.O. Box 1970 Richland, WA 99352
A Subsidiary of Westinghouse Electric Corporation
Prepared for the U.S. Department of Energy
under Contract No. DE-AC14-76FF02170

Operated by
Westinghouse
Hanford Company
for the U.S. DOE

A Subsidiary of
Westinghouse Electric
Corporation

Contract No.
DE-AC14-76FF02170

P.O. Box 1970
Richland, WA 99352

Hanford Engineering Development Laboratory

INFORMATION CONCERNING USE OF THIS DOCUMENT

CONTROLLED DISTRIBUTION DOCUMENT

This is a working document required for internal Hanford Engineering Development Laboratory (HEDL) use and program distribution in order to perform, direct or integrate the work of the U.S. Department of Energy (DOE) programs. Distribution is limited to HEDL, DOE and DOE contractors who require the document in order to perform work under Contract DE-AC14-76FF02170 for HEDL or DOE. Its contents shall not be published, further disseminated or used for other purposes until approval for such release or use has been secured from the Supervisor, HEDL Central Files.

PATENT STATUS

This document copy, since it is transmitted in advance of patent clearance, is made available in confidence solely for use in performance of work under contracts with the U.S. Department of Energy. This document is not to be published nor its contents otherwise disseminated or used for purposes other than specified above before patent approval for such release or use has been secured, upon request, from the RL Patent Attorney, Richland Operations Office, U.S. DOE, Richland, Washington 99352.

NOTICE

This document was prepared as an account of work sponsored by the United States Government. Neither the United States nor the U.S. DOE, nor any of its employes, nor any of its contractors, subcontractors or their employes, makes any warranty, expressed or implied, or assumes any legal liability or responsibility for any third party's use or the results of such use of any information, apparatus, product or process disclosed in this report, or represents that its use by such third party would not infringe privately owned rights.

PRELIMINARY DOCUMENT

This document contains information of a preliminary nature prepared in the course of work under U.S. DOE Contract DE-AC14-76FF02170. This information is subject to corrections or modification upon the collection and evaluation of additional data.

Hanford Engineering Development Laboratory

P.O. BOX 1970 RICHLAND, WA 99352

8151165

April 8, 1981

Dr. Ron Manvi
Task Manager
Thermal Storage
Advanced Solar Thermal Technology
Jet Propulsion Laboratory
4800 Oak Grove Drive
Pasadena, CA 91103

SENSIBLE AND LATENT HEAT BUFFER STORAGE RECEIVER SYSTEMS FOR DISH MOUNTED SOLAR APPLICATIONS (TC-1893)

Attached for your information is the final report on "Sensible and Latent Heat Buffer Storage Receiver", TC-1893, prepared by HEDL for JPL Thermal Storage Division on contract number WO-8693, NAS7-100.

E. M. Sheen, Manager
Instrument Technology

spw

DISTRIBUTION

JPL (26)

R. Manvi (25)
J. Walsh

DOE/RL

M. Plahuta

FTFF/PO

H. Ranson

HEDL (52)

S. W. Berglin	W/A21	(5)
M. B. Boone	W/A21	
R. W. Davis	W/E19	(10)
D. R. Green	W/A56	(10)
I. F. Marshall	W/C125	(2)
M. P. Nolan	W/D26	(2)
L. S. Price	W/A56	(10)
E. M. Sheen	W/A56	(5)
J. M. Yatabe	W/C22	
Central Files	W/C110	(5)
Publication Services	W/C112	(2)

TC-1893

SENSIBLE AND LATENT HEAT BUFFER STORAGE RECEIVER SYSTEMS FOR DISH MOUNTED SOLAR APPLICATION

Hanford Engineering Development Laboratory

Prepared by
R.W. Davis
D.R. Green
M.P. Nolan
L.S. Price
February 1981

HANFORD ENGINEERING DEVELOPMENT LABORATORY
Operated by Westinghouse Hanford Company
P.O. Box 1970 Richland, WA 99352
A Subsidiary of Westinghouse Electric Corporation
Prepared for the U.S. Department of Energy
under Contract No. DE-AC14-76FF02170

FORWARD

This report focuses on concepts developed by the Hanford Engineering Development Laboratory (HEDL) on high temperature solar buffer receivers for use with a parabolic dish solar system. The work was carried out under a Department of Energy Solar Thermal contract managed through the Jet Propulsion Laboratory. Dr. Ram Manvi - Task Manager, Jet Propulsion Laboratory, Contract Number NAS7-100 DPRWO-8693.

TABLE OF CONTENTS

List of Symbols

A_p = cross sectional area of a gas passage (cm^2)
A_{SA} = surface area of a gas passage (cm^2)
ajb = various radii of the system (cm)
C = specific heat (cal gm^{-1} $°C^{-1}$)
D = equivalent thickness of "fin" (cm)
d = diameter of tubular gas passage (cm)
F_o = heat flux at the surface of the graphite cylinder (W cm^{-2})
G = mass velocity (gm sec^{-1} cm^{-2})
g = acceleration due to gravity (cm sec^{-2})
H = surface heat transfer coefficient
H_F = flat plate "fin" surface heat transfer coefficient (cal cm^{-2} sec^{-1} $°C^{-1}$)
H_p = heat transfer coefficient for the gas passages (cal cm^{-2} sec^{-1} $°C^{-1}$)
I.D. = inside diameter (cm)
J_N = Bessel functions
K = thermal conductivity (cal cm^{-1} sec^{-1} $°C^{-1}$)
K_A = thermal conductivity of air at 1160°C and 3 atmospheres pressure (cal cm^{-1} sec^{-1} $°C^{-1}$)
L = radial thickness of the heat exchanger (cm)
l = wall thickness of the core enclosure (cm)
ℓ = length of the heat exchanger (cm)
$\dot{m}$ = mass flow rate of the working fluid-air (gm sec^{-1})
$\dot{m}_p$ = mass flow rate through a single gas passage (gm sec^{-1})
N = Reynolds number
O.D. = outside diameter (cm)
P = pressure drop (dynes/cm^{-2})
P_o = power (kW)
P_{in} = radiant input to the sapphire window of the core (kW)
P_{out} = re-radiation loss from the sapphire window (kW)
Q = heat flow (kW)
Q_T = total thermal output (kW)
q heat flux (W cm^{-2})
r = radius of the graphite core (cm)
T = temperature of the graphite core (°C)
T_o = initial (charged) temperature of the core (°C)
T_s = temperature at the outer surface of the core (°C)
ΔT = change in temperature of the working fluid (°C)
t = time (sec)

List of Symbols (continued)

U_A = average gas velocity in the heat exchanger (cm sec^{-1})
u = velocity (cm sec^{-1})
V_G = volume of the graphite core (cm^3)
V_L = temperature at the outer periphery of the heat exchanger (°C)
V_o = temperature of the core container/heat exchanger interface (°C)
$\dot{V}p$ = volumetric flow rate through a gas passage (cm^3 sec^{-1})
X = variable radial distance along a "fin" (cm)
α = thermal diffusivity (cm^2 sec^{-1})
γ = specific weight (dynes cm^{-3})
ε = emissivity
μ = viscosity (poise)
ρ = density (gm cm^{-3})
ρ_A = density of air at 1160°C and 3 atmospheres pressure (gm cm^{-3})
σ = Stefan-Boltzman constant (W cm^{-2} deg^{-4} sec^{-1})

List of Figures

List of Tables

ADVANCED HIGH TEMPERATURE SOLAR BUFFER RECEIVER PROGRAM

I. INTRODUCTION

A parabolic dish will focus the sun's radiant energy onto a heat receiver unit. This receiver transfers the radiant heat energy to a turbine/generator system by means of a working gas (air at 45 psia). The buffer storage of the receiver is needed to transfer stored solar heat energy to the working gas during cloudy periods. This system will allow operation of the turbine/generator for up to 30 minute intervals.

HEDL has conceived two suffered solar receiver systems to fulfill this task. One concept uses storage of latent heat in molten silicon while another uses sensible heat storage in solid graphite. Both concepts meet the necessary requirements and advance the area of high temperature thermal storage.

The description, operation, material properties, background history and parameters of the above concepts are presented in this report. Table 1 shows a comparison between HEDL heat receiver concepts and previous technology. Design performance characteristics were computed for the sensible heat storage device concept. This emphasis on the sensible heat concept was decided at a December 1980 program review meeting between HEDL and JPL personnel. Detailed design performance computations were beyond the scope of the present work for the latent heat case.

A. Concept Requirements

The baseline design criteria for HEDL's advanced high temperature buffer storage concepts are listed in Table 2 along with the temperatures and heat flow calculated for the HEDL systems.

High temperature materials used to contain the storage core and transfer heat energy to the gas must have high thermal conductivity, good mechanical strength, and oxidation resistance. Careful material selection for each

TABLE 1

COMPARISON BETWEEN HEDL HEAT RECEIVER CONCEPTS
AND PREVIOUS TECHNOLOGY

PREVIOUS TECHNOLOGY	HEDL LATENT HEAT BUFFER SOLAR RECEIVER (Si)	HEDL SENSIBLE HEAT BUFFER SOLAR RECEIVER (GRAPHITE)
3 minute buffer storage	>30 minute buffer storage	>30 minute buffer storage
Low heat storage to mass ratio of storage material (40 cal/gm)	High heat storage to mass ratio of storage material (431 cal/gm)	High heat storage to mass ratio of storage material (200 cal/gm)
One quartz window	No window required	One quartz window One sapphire window
Uncontrolled outlet temperature	Uncontrolled outlet temperature	Controlled outlet temperature
Uncontrolled charge rate	Uncontrolled charge rate	Controlled charge rate
Solid core during normal operation	Liquid core during normal operation	Solid core during normal operation
No moving parts	One moving part	One moving part
Maximum output of stored energy limited to maximum insolation	Maximum output of stored energy limited to maximum insolation	Maximum output of stored energy can be controlled to exceed maximum insolation for short periods if desired
Direct contact between air and storage medium	Argon pressurization required around core	Argon pressurization required around core

TABLE 2

RECEIVER DESIGN REQUIREMENT CHARACTERISTICS SUMMARY

DESIGN CHARACTERISTICS	JPL REQUIREMENTS	HEDL SENSIBLE BUFFER HEAT RECEIVER	HEDL LATENT BUFFER HEAT RECEIVER	PRESENT HEAT RECEIVER SYSTEM
Inlet gas temp.	950°C	950°C	950°C	950°C
Outlet gas temp.	1370°C	1370°C	1370°C	1370°C
Gas Pressure	45 psia	45 psia	45 psia	45 psia
Maximum Δ Pressure	4%	0.299%	0.06%	1.4%
Gas Type (Working Fluid)	Air	Air	Air	Air
Max. Δ temp. of outlet gas	1170 - 1370°C	1170 - 1370°C	1170 - 1370°C	1170 - 1370°C
Storage Time	30 min.	> 30 min.	> 30 min.	3 min.
Receiver Mass	150 - 200 kg	∿ 200 kg	∿ 160 kg	141 kg
Mass flow of gas for 60 kw output	130 g/sec	130 g/sec	130 g/sec	114 g/sec

component is necessary to meet the criteria of the buffer heat receiver. Tables 3, 4, and 5 give a summary of the materials and key properties on which HEDL's receiver concepts were based.

The evaporation rate and oxidation rate of graphite and silicon carbide, respectively, were calculated at the temperature of application from values found in the literature. In both cases, the rates determined were sufficiently low so as to indicate no problems with receiver operation over several years time.

B. Background Information

There have been many materials used for energy storage applications covering a large temperature range. Only a few storage materials can meet the requirements of a buffer thermal storage system for high temperature operation (>1400°C). The material must have a high thermal conductivity (solid, liquid or both), be abundant and inexpensive, and give a high heat storage to mass ratio. In addition, latent heat storage candidates face problem areas of containment, solidification control, corrosion, and environmetal hazards.

In the sensible heat storage material, a high heat capacity is required to give a high energy storage to mass ratio. High temperatures are necessary due to the time (30 min.) during which an outlet temperature greater than 1170°C must be maintained. The thermal conductivity and configuration of the core determines how fast the heat can be withdrawn without excessive radial temperature drop. In addition, mechanical strength and creep resistance at high temperature are important.

In the HEDL sensible heat concept shown in Figure 1, graphite has been chosen as a core material since it meets all these criteria. A key property of the graphite is its increase in heat capacity and mechanical strength at high temperature.

TABLE 3

KEY MATERIAL PROPERTIES

MATERIAL	USE (°C)	EVAPORATION RATE (mm/yr)	TENSILE STRENGTH (10^6 N/m^2)	COMPRESSIVE STRENGTH (10^6 N/m^2)	DENSITY (gm/cm^3)	HEAT CAPACITY (cal/gm-°C)	THERMAL CONDUCTIVITY (cal/cm-sec-°C)	EMISSIVITY	THERMAL EXPANSION COEFFICIENT (10^{-6}/°C)
Graphite	2482 inert atm. (1)	0.01415 at 1800°C in vacuo (2)	22.05-35.77 at 1927°C (3)	49-73.5 at 1800°C (4)	1.4-1.7 (5)	0.485-0.5 1400-1800°C (6)	0.072 at 1800°C (7)	Normal Total 0.8 - 0.85 from 1400°C-1800°C (8)	5.2-6.2 at 1800°C (9)
BN	Stable up to 1927 inert atm. (10)		7.9236 at 1800°C (11)	234.3-310.0 at r.t.* (12)	2.25 (13)	0.475 from 1400-1800°C (14)	0.049 at 1800°C (15)	Normal Total $\simeq$ 0.77 at 1000°C *(16)	9.3, 0-1400°C 45, 1400-1600°C 65, 1600-1800°C (17)
B_4C	m.p.→2454 reacts with O_2 above 982 (18)		155.0 at 980°C * (19)	2852 at r.t. * (20)	2.53 (21)	0.61 at 1800°C (22)	0.036 at 1800°C (23)	(λ = 65μ) 0.86 from 1400-1800°C (24)	7.4 from 1000-1800°C (25)
SiC	1649 in oxidizing atm. (26)	0.0959 at 1500°C in air (27)	1826 at 982°C * (28)	565-827 at r.t. * (29)	3.2 (30)	0.325 at 1400°C (31)	0.04 at 1400°C (32)	Normal Total 0.8 at 1400°C (33)	5.5 from 1000-1400°C (34)
Al_2O_3	1980 in air (35)	0.203 at 1527°C in vacuo (36)	29.63 at 1400°C (37)	245.3 at 1400°C (38)	3.73 (39)	0.31 from 1400-1800°C (40)	0.014 at 1400°C (41)	Hemispherical total 0.56 at 100°C * (42)	10.75 from 1000-1400°C (43)
Quartz	In air: 899 continuous service 1260 for short-term exposure (44)		62.1 at r.t. * (45)	1166 at r.t. * (46)	2.3 (47)	0.179 at r.t. * (48)	0.018 at 1000°C (49)	Hemispherical total 0.76 at 39°C * (50)	1.2 from 500-1000°C (51)
Cera Form (primarily mullite)	1427 (52)				0.352 (53)		0.000123 426°C Mean (54)		
Fiber Form (primarily graphite)	2482 inert atm. (55)	(graphite) 0.01415 at 1800°C in vacuo (56)		>1.378 r.t. * (57)	0.17-0.25 (58)	(graphite) 0.485-0.5 1400-1800°C (59)	0.00106 at 1800°C (60)	greater than 0.9 (61)	4.7 from 1440-1715°C (62)

* Value not available at expected operating temperature.

TABLE 4. SELECTION OF MATERIALS FOR SENSIBLE HEAT RECEIVER

APPLICATION	MATERIAL	CRITERIA	KEY PROPERTIES	REASON FOR SELECTION
Storage Core	Graphite, Boron Carbide, Boron Nitride	High heat storage/mass ratio	Heat storage (cal/gm°C) Graphite 0.5 B_4C 0.61 BN 0.475	BN - high heat storage/mass ratio Graphite - strength increases with temperature - inexpensive - high heat storage/wt ratio B_4C - high heat storage/wt ratio - abundance
Movable Insulation Shield	Fiberform (Graphite)	Compatible with core - low thermal conductivity - low thermal expansion, rigid at high temperature.	Thermal Expansion 4.7×10^{-6}/C°) Thermal Conductance (cal/cm sec C°) 0.00106 at 1800°C	Ease of fabrication; inexpensive; rigid.
Insulation Shield Retractor	Graphite Tube	Compatible with core Strong at high temperatures.	Tensile Strength at 1927°C 22.05 - 35.77 $\times 10^6$ N/m^2 (3.2 - 5.2 $\times 10^3$ psi) Compressive Strength at 1800°C 49.0 - 73.5 $\times 10^6$ N/m^2 (7.11 - 10.7 $\times 10^3$ psi)	Easily fabricated; strong at high temperature.
Core/Shield Envelope	Silicon Carbide	Good heat transfer Compatible with movable shield Low oxidation rate Shock resistance	Oxidation Rate 0.0678 mm/year at 1500°C Thermal Expansion: 4.4 - 5 $\times 10^{-6}$/C° Tensile Strength at 982°C* 1826 $\times 10^6$ N/m^2 (265.0 $\times 10^3$ psi) Thermal Conductivity (cal/cm sec C°) 0.04 at 1400°C	Fabrication ease for large shapes; good shock resistance; good oxidation resistance at high temperatures.

(continued)

Table 4 (Cont'd)

APPLICATION	MATERIAL	CRITERIA	KEY PROPERTIES	REASON FOR SELECTION
Heat Exchangers	Silicon Carbide	Heat transfer Low oxidation rate Thermal shock resistance	Oxidation Rate 0.0959 mm/yr at 1500°C Thermal Conductivity 0.04 cal/cm^{-1} $sec^{-1}C°^{-1}$	Fabricable in a honeycomb structure; good shock resistance; low oxidation rate
Reinforcing Rods	Silicon Carbide	Shock Resistance Low oxidation rate High compressive strength	Oxidation Rate 0.0384 mm/yr at 1400°C Compressive Strength	Good shock resistance; good compressive strength
Gas Flow Baffle	Silicon Carbide	Thermal Shock Resistance Oxidation Rate	Oxidation Rate 0.0178 mm/yr at 1200°C	Fabrication case for large shapes; good thermal shock resistance; low oxidation rate
Core Window	Sapphire	Optical Characteristics Compatible with air at high temperatures	Transmissivity - High Absorption - Low	Will not react with air at high temperatures; transmits visible light
High Temperature Insulation	Cera-Form	Compatible with air at high temperatures Compatible with SiC Low thermal conductivity	Oxidation Rate Thermal Conductivity (cal/cm °C sec) 0.000123 at 426°C mean	Compatible with air; low thermal conductivity; compatible with SiC.
Bellows	Stainless Steel or other Corrosion Resistant material		Inexpensive Flexible	

Table 4 (Cont'd)

APPLICATION	MATERIAL	CRITERIA	KEY PROPERTIES	REASON FOR SELECTION
Receiver Window	Quartz	Compatible with air at high temperature Optical Requirements	Transmissivity Absorption	Compatible with air at high temperatures; transparent to visible light; opaque to certain bands of infrared.
Structural Mounting Vessel	Steel	Tensile Strength Corrosion Resistance	Properties Variable	Well understood material for low temperatures; inexpensive; easily machined
Insulation	Fiberform (Graphite)	Compatible with core - low thermal conductivity - low thermal expansion, rigid at high temperature.	Thermal Expansion $2.7 \times 10^{-6}/C°$ Thermal Conductance (cal/cm-sec-C°) 0.00106 at 1800°C	Ease of fabrication; inexpensive; rigid; low thermal conductivity at high temperatures

TABLE 5

MATERIAL SELECTION FOR THE SILICON LATENT HEAT RECEIVER

APPLICATION	MATERIAL	CRITERIA	KEY PROPERTIES	REASON FOR SELECTION
Molten Silicon	Silicon	Melting Point High Thermal Conductivity Latent Heat of Fusion	Thermal Conductivity at 1412°C 0.0526 cal/cm-°C-sec Latent Heat of Fusion 431/cal/gm	Melts in Operation Temp. Zone High Latent Heat of Fusion High Thermal Conductivity
Silicon Containment	Boron Nitride	Compatible with Graphite at High Temperature Resistant to Attack by Molten Silicon	Heat Capacity From 1400 - 1800°C 0.475 cal/gm-°C	Not Wetted by Molten Silicon Pressed Material has Great Strength and is Stable to 1927°C in Inert Atmosphere
Frame	Graphite	Sturdy at High Temperatures Compatible With BN at High Temps. Thermal Conductivity	Compressive Strength at 1800°C 49.0 - 73.5 x 10^6 N/m^2 (7.11 - 10.7 x 10^3 psi) Thermal Conductivity 0.072 cal/cm sec °C at 1800°C	Strength Increases With Temperature Easily Molded Good Thermal Conductor
Insulation	Fiberform	Low Thermal Conductivity	Thermal Conductivity at 1800°C 0.00106 cal/cm-sec-°C	Very Low Thermal Conductivity Can be Fabrication to Specifications
Housing	Silicon Carbide	Sturdy at High Temperature	Thermal Conductivity at 1400°C 0.04 cal/cm-°C-sec	Retains its Strength at High Temperatures Has a Low Thermal Expansion Good Thermal Conductivity
Support Cradle	Silicon Carbide	Sturdy at High Temperature	Thermal Conductivity at 1400°C 0.04 cal/cm-°C-sec	Retains its Strength at High Temperatures Has a Low Thermal Expansion Good Thermal Conductivity

SENSIBLE HEAT BUFFER STORAGE DEVICE FOR DISH MOUNTED RECEIVERS

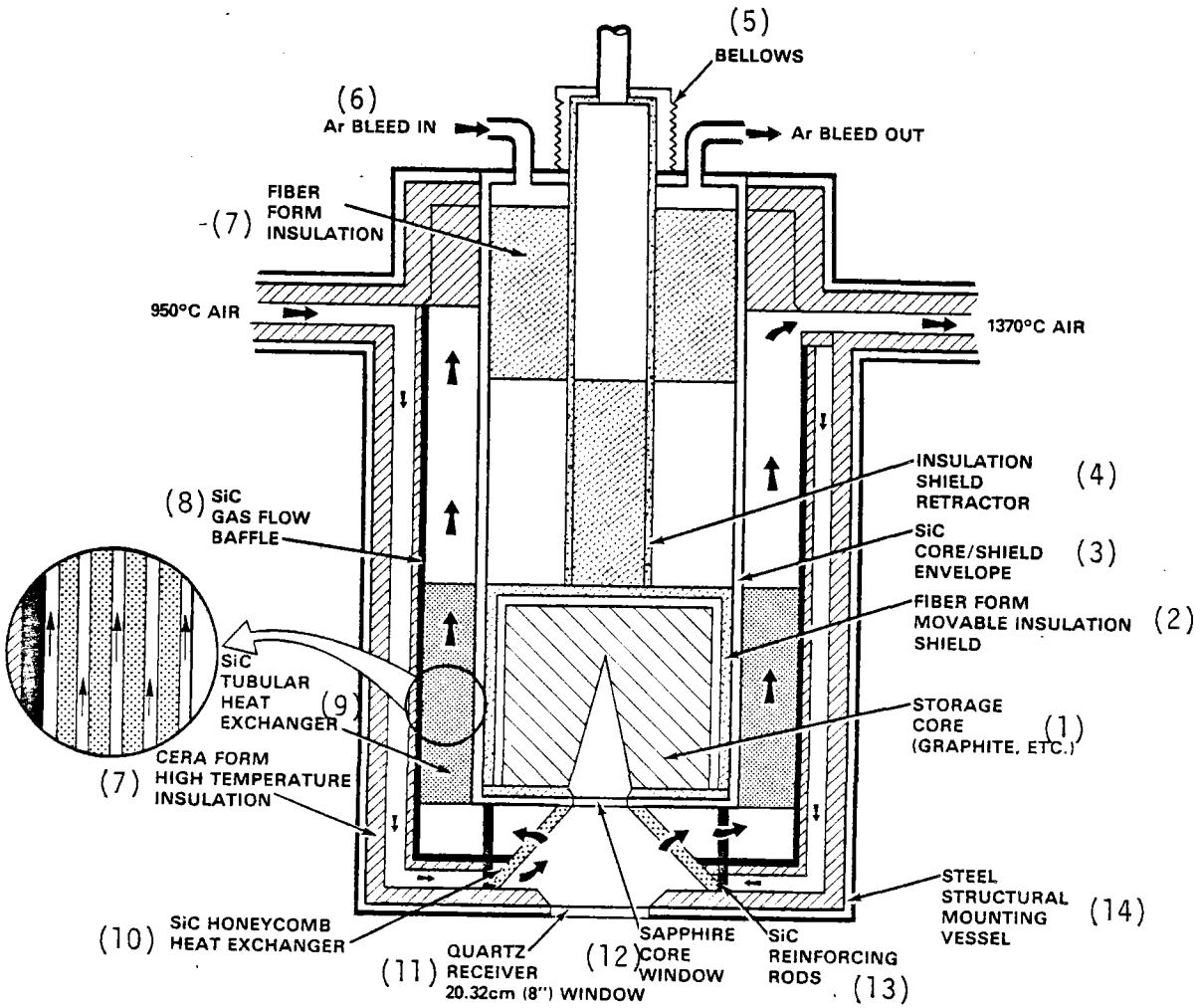

FIGURE 1: CONCEPTUAL DESIGN

HEDL 8102-098.1

In the latent heat storage material, a high thermal conductivity in the solid phase and material compatibility become important. The thermal conductivity of the solid phase must be high so that effective heat transfer from the interface with the molten materials can take place as energy is withdrawn. The reaction of the storage medium with its container must remain low for long periods of time at high temperatures. Thermal cycling will take place in a buffer receiver therefore, thermal expansion and bonding or lack of bonding between the storage material and container play major roles.

HEDL's latent heat storage concept uses silicon as its storage media. Silicon was chosen because of its high latent heat of fusion, its melting point, and its thermal properties. Unlike molten salts and other latent storage candidates, silicon expands on solidification. Its thermal conductivity is high in both solid and liquid phases so solidification control is not necessary to transfer the heat energy to the working gas. Silicon does not react with wet boron nitride, so boron nitride was chosen as the containment material. The design of the apparatus is shown in Figures 2 and 3 and will be described in detail in a later section.

II. BUFFER STORAGE CONCEPT USING SENSIBLE HEAT MATERIAL

A. Description

The sensible heat receiver is composed of the following components (refer to Figure 1):

(1) A solid storage core to contain the deposited solar energy for use during cloud cover conditions.

(2) A movable insulation shield to control the rate of heat transfer from the core to the working gas.

(3) A core/shield envelope to aid in core support and to prevent the working gas from coming in contact with the core/shield area.

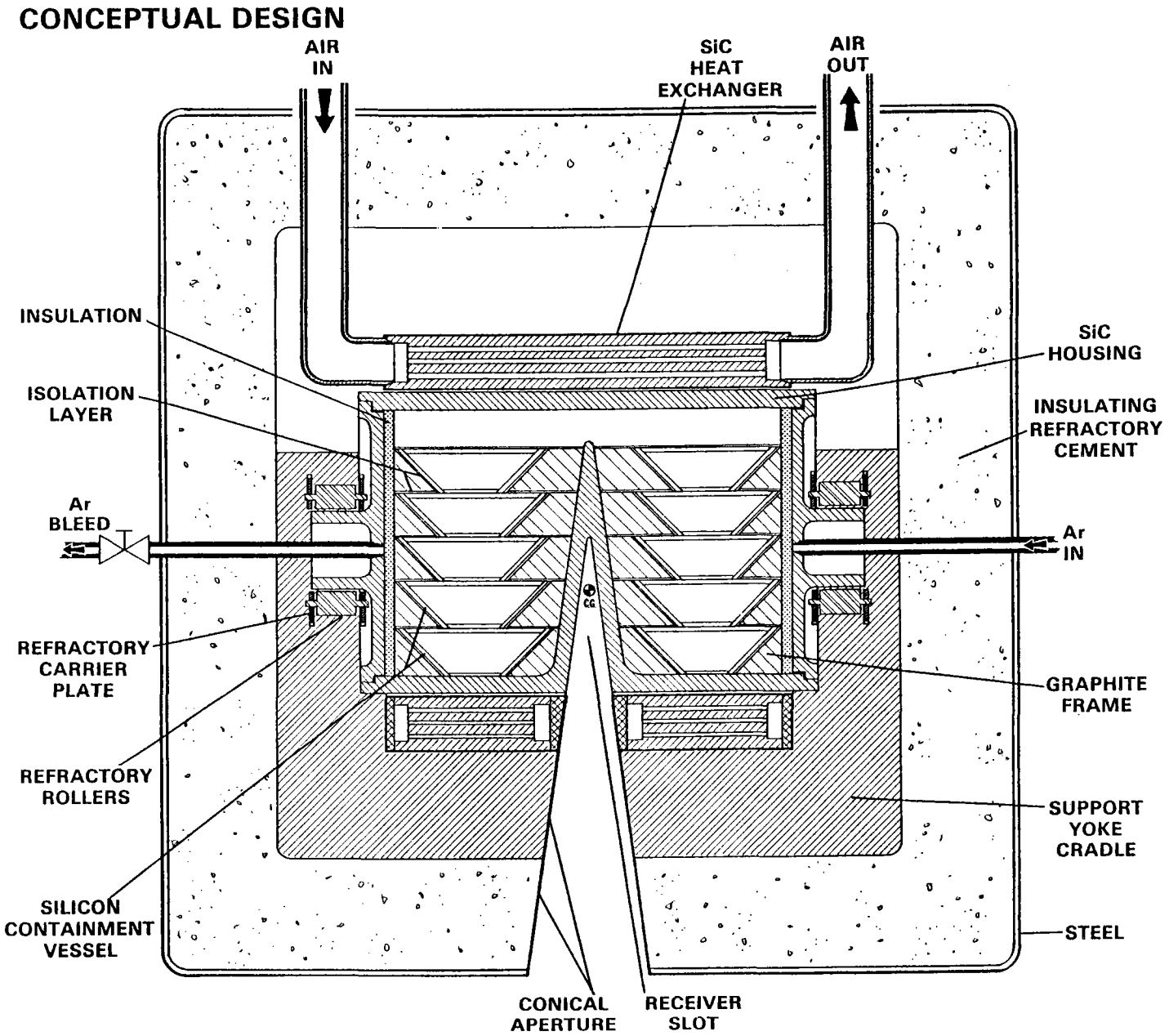

FIGURE 2: SILICON LATENT HEAT STORAGE DEVICE

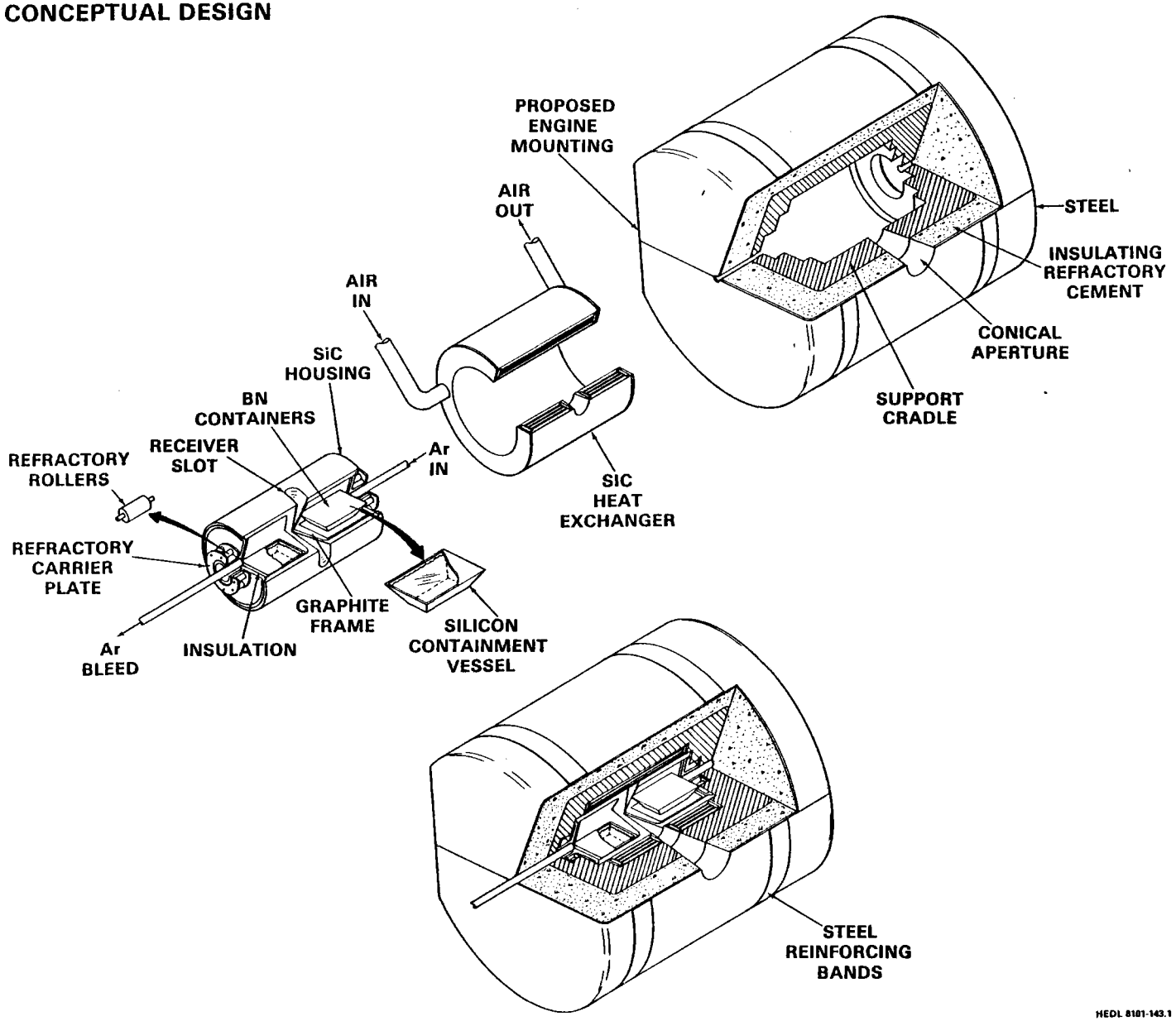

Figure 3. Pictorial View of the Silicon Latent Heat Storage Device

(4) An insulation shield retractor and bi-metal, gas expansion or other type of device to allow control of the movable shield to maintain constant outlet gas temperature.

(5) A bellows to allow shield retraction.

(6) An inert gas bleed system to provide positive pressure of inert gas in the core/shield container preventing the pressurized working gas from entering the core/shield region.

(7) Insulation to minimize heat leakage.

(8) A gas baffle to direct the working gas flow.

(9) A heat exchanger with tubular gas passages to transfer the storage core heat energy to the working gas.

(10) A honeycomb heat exchanger to gather solar energy and transfer it directly to the working gas.

(11) A quartz window to allow concentrated solar energy to be deposited in the receiver.

(12) A sapphire window to allow some of the solar energy to be deposited on the core surface.

(13) Reinforcing rods to help support the receiver inner components.

(14) A steel structural vessel to house and provide mounting for the buffer heat receiver and to contain the working gas.

B. Operation

A normal daily working cycle of the graphite solar heat receiver comprises the following events (refer to Figure 1):

1. For initial startup, the movable insulation shield will be closed and the working air will be circulated through the receiver via a closed recirculation loop.

2. At sunrise, the parabolic dish mirror will be turned toward the sun focusing the sunlight onto the receiver quartz window aperture depositing heat energy in the graphite heat storage core and the SiC honeycomb heat exchanger structure.

3. The recirculating air increases in temperature as it flows through the honeycomb heat exchanger structure. When the recirculating air temperature exceeds the temperature of the graphite storage core surface, the movable shield is fully retracted allowing heat energy to transfer from the gas to the core via the heat exchanger.

4. When the recirculating air temperature reaches 1370°C, the recirculating line is altered allowing the hot air to start the turbine. The air entering the receiver is now at a lower temperature than 1370°C allowing heat transfer from the graphite core to the air.

5. The receiver outlet air will be maintained at a temperature of 1170°C by regulating the heat transfer rate from the core to the air via the movable shield allowing the core to continue charging.

6. When the core reaches its fully charged capacity, the core temperature will be held at a constant 1800°C via the movable shield.

7. If insulation is restricted by temporary cloud cover, the movable shield will be withdrawn as necessary to maintain power at the receiver outlet. This operation will continue until the shield is fully retracted (> 30 minutes later).

8. If at this point no insolation is present, the turbine will be shut down and the movable shield will be closed to conserve core heat energy.

9. When insolation again occurs, the air recirculation line is re-established allowing the air to reach 1370°C once again.

10. Once the gas reaches a temperature of 1370°C, the recirculation line is closed and the turbine begins operation. The movable shield of the receiver is regulated accordingly and the cycle continues.

11. At sunset, heat is transferred from the core to the air until the movable shield is fully retracted. At this point the turbine is shut down and the shield is fully closed to minimize heat energy loss from the storage core until the following morning.

C. Computed Design Performance Characteristics

This sub-section summarizes the performance characteristics of the graphite storage core as determined from initial design computations. These computations, described in detail in the appendix, are approximations based on analytical solutions. The following assumptions were necessary:

1. Uniform distribution of the heat flow over the entire storage core surface.

2. Uniform core surface temperature equal to the longitudinal average temperature on the surface of the core.

3. Heat exchanger and gas stream radial zone temperatures are equal to the longitudinal average temperature in each zone.

4. The surface temperature of the core during discharge is the result of a heat flow equal to the steady 45.5 kW average of the high (60 kW) and low (31 kW) design points.

5. The core is long and slender to prevent expensive radial temperature drop. (Later designs using computer analysis can incorporate shorter,

larger diameter specially shaped cores. Figure 4 depicts one such possible design)

6. Insolation entering the receiver windows is assumed to be at peak value.

Computer programming to solve the complex interactions between convection, wall temperature, radial time-temperature transients, radiation transfer, position of the movable shield and re-radiation losses through the window will be necessary during final design. Such programming was beyond the scope of the present work, which was intended only to yield a conceptual design.

Initial operation requires that the movable insulation shield be in the up position (open) to allow heat to flow into the core from the recirculating air as mentioned above. When the outlet air temperature has reached 1370°C, the insulation shield closes far enough to allow the core to continue charging while operating the turbine at the minimum air temperature (1170°C) and power (31 kW). As seen in the Appendix, the peak input to the Al_2O_3 core window (neglecting reflection and transmission losses) is 38 kW, while the re-radiation loss is less than 5 kW. Hence the movable shield will have to be left partially open even while charging the core. A heat flow of 9 kW from the core to the heat exchanger will sustain the minimum operating power of 31 kW to the turbine. Therefore, 29 kW would be used to charge the core and balance re-radiation losses. As the core approaches its maximum design temperature (1800°C), the insulation shield is retracted far enough to maintain a heat balance so the energy flow to the working gas plus re-radiation and other losses equal the energy input to the core through the Al_2O_3 window. Radial temperature drops through the differing wall thicknesses of the core's conical radiation cavity are assumed negligible.

Assume the core is uniformly charged to 1800°C at the beginning of discharge, and that some method such as a tapered, slotted or layered movable shield has been provided. This allows a uniform flow of heat over the entire core area at a rate controlled to vary linearly from 60 kW to 31 kW over

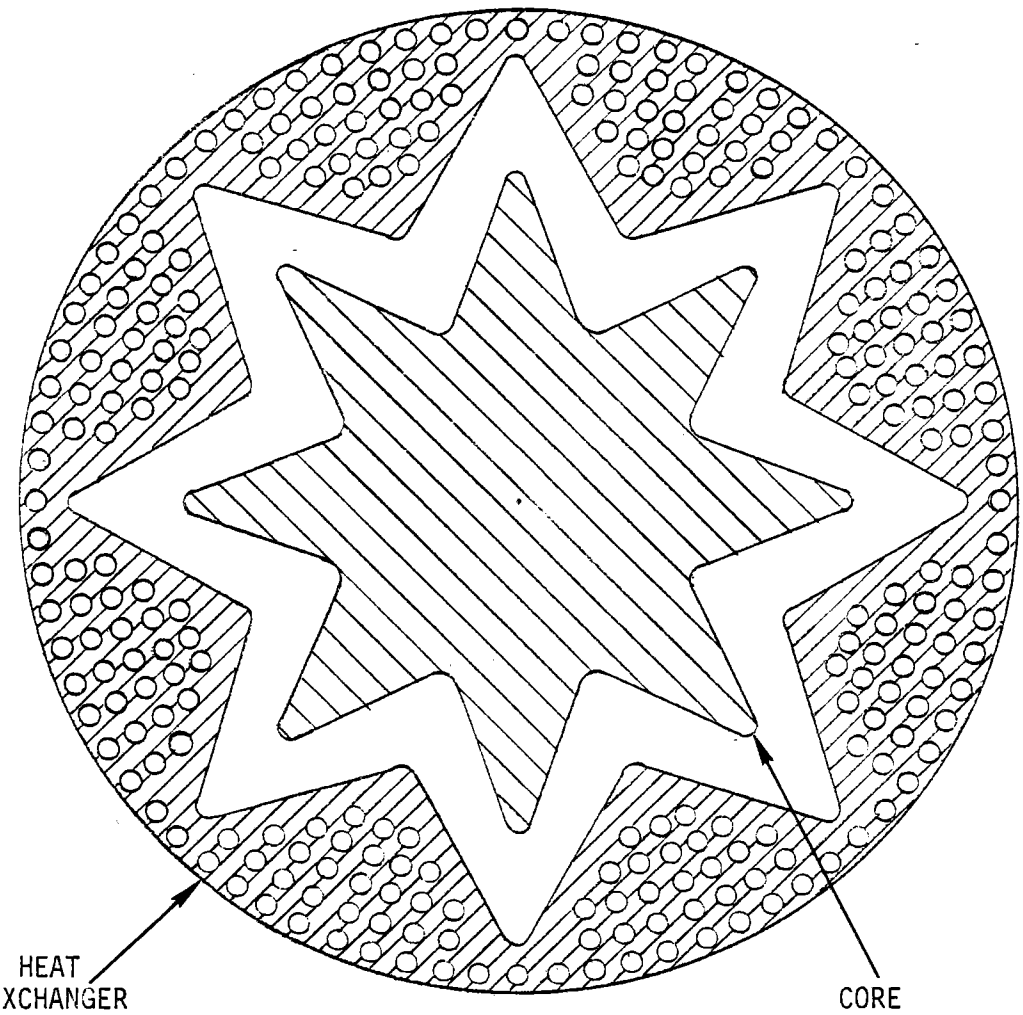

FIGURE 4. Advanced Graphite Storage Core Design.

the 30 minute discharge time. Computations of the approximate temperatures at key points mid-length along the assembly are illustrated in Figure 5 for times near the beginning and end of discharge. With the movable insulation shield fully retracted, radiant heat transfer through the core-to-containment vessel gap would exceed the required rate, even at the end-point of discharge. Hence, the shield is not fully open even after 30 minutes and a safety margin of storage for an additional time is available.

A modest air pressure drop through the heat exchanger of 9.04×10^2 dynes/cm^2 (0.130 lb/in^2) was computed at maximum power flow conditions which is well within the required 4% limit. End aperture losses (pressure drops) should also be small.

III. LATENT HEAT BUFFER STORAGE

A. Description

The latent heat receiver is composed of the following components (refer to Figures 2 and 3):

1. A latent heat storage core (silicon) to retain the deposited solar energy for use during cloud cover conditions.

2. A core container material (boron nitride) to contain the molten silicon.

3. A graphite frame to house and support the core container.

4. A multipurpose container to aid in support and prevent oxygen interaction with the core components. This container also keeps the silicon upright during sun tracking. The housing is cylindrical shaped with an aperture for solar energy desposition.

5. An argon bleed to flush oxygen from the core and prevent oxidation at high temperatures.

6. A heat exchanger to transfer the heat energy to the working fluid (air).

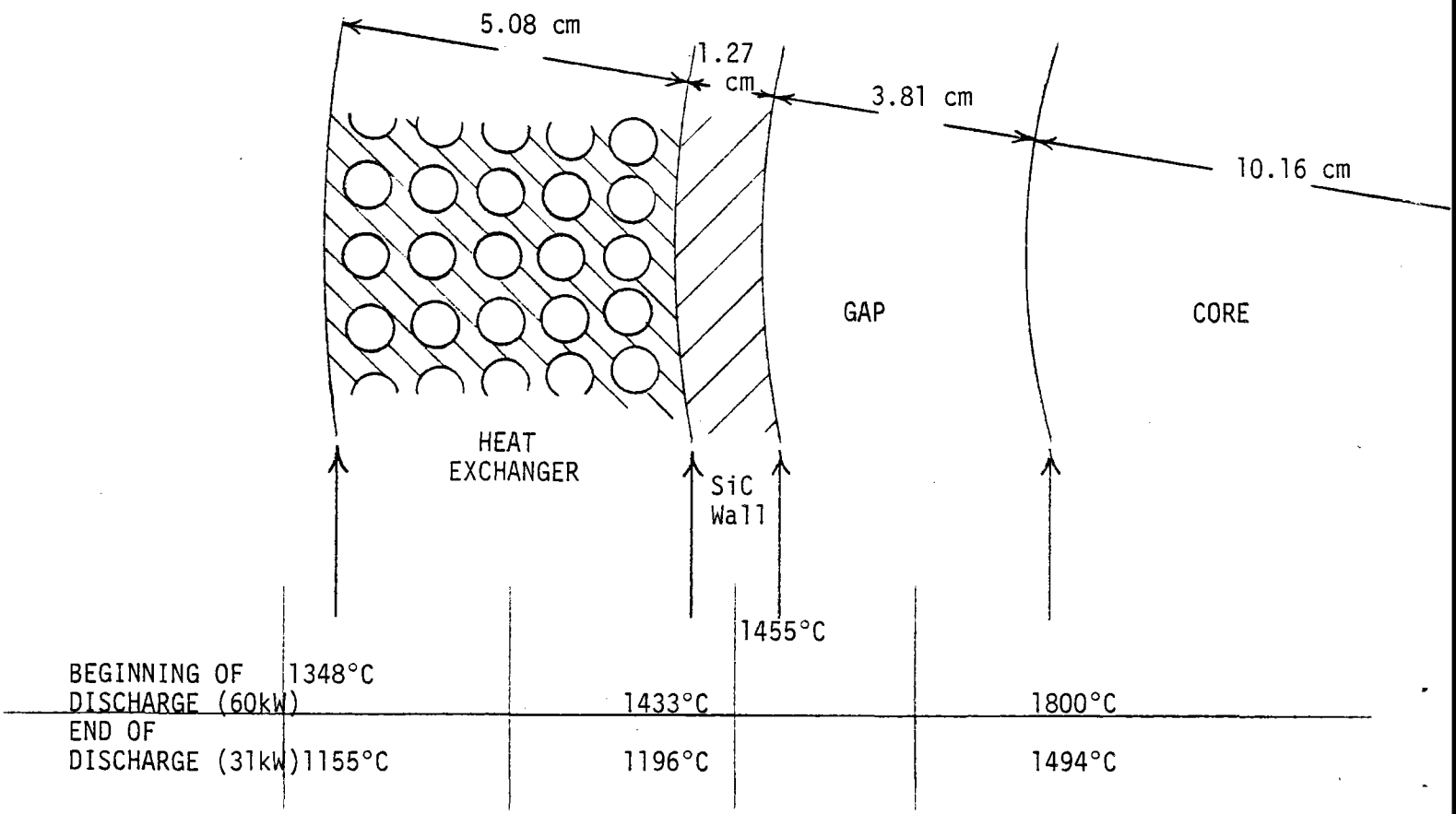

FIGURE 5. Calculated Temperatures at Various Points in the Graphite Buffer Heat Receiver.

7. Refractory bearings to allow free movement of the core.

8. A support yoke to provide bearing and core component support.

9. A refractory cement to minimize heat loss and provide support for all receiver components.

10. A steel outer shell to allow for receiver mounting.

B. Operation

A normal daily working cycle of the silicon solar heat receiver comprises the following events (refer to Figures 2 and 3):

1. At sunrise, the parabolic dish mirror will be directed toward the sun focusing the sunlight into the receiver conical aperture.

2. This heat energy will be deposited in the receiver slot of the SiC housing. This housing is of a cylindrical design suspended on refractory roller bearings allowing the silicon containment vessels to remain level as the dish tracks the sun.

3. Heat is transferred from the receiver slot through the graphite frames and boron nitride containers into the silicon.

4. The temperature of the silicon rises to 1412°C and melting begins.

5. After the silicon has melted and the temperature reaches 1425°C, air will be recirculated through the SiC heat exchanger until a temperature of 1370°C is obtained. At 1370°C air temperature, the recirculating line is altered and the turbine is started.

6. If insolation is restricted by temporary cloud cover, the silicon will begin to solidify and transfer its stored energy into the air via the heat exchanger for up to a 30-minute duration.

7. If, at this point, no insolation is present, the turbine will be shut down.

8. When insolation again occurs heat is transferred to the silicon, melting it.

9. Upon a rise in silicon temperature above 1412°C, air is recirculated and normal operation will continue as above.

IV. CONCLUSIONS, RECOMMENDATIONS, AND FUTURE WORK

HEDL has chosen graphite as the sensible heat storage material. Graphite high temperature properties are well documented in the literature. The material is inexpensive, abundant in the U.S., and has exceptional characteristics for use in a high temperature energy storage system. Graphite's mechanical strength, thermal conductivity, and heat capacity are excellent at high temperatures. The evaporation rate at 1800°C is low, preventing excessive deposition of core material on the cooler containment surfaces. The HEDL design is a significant improvement over present technology.

Although graphite was chosen in the conservative HEDL design, other materials of which the high temperature properties are not as well known should be investigated. Materials with higher heat capacity such as boron carbide, boron nitride and beryillium carbide should be scrutinized where cost and abundance do not play major roles. Some of these materials could provide a factor of two greater storage/mass ratio than graphite and a factor of 10 over previously used materials.

Silicon was chosen for the latent heat storage material due to its excellent heat storage to mass ratio and its high thermal conductivity in both the solid and liquid phases. The literature indicates silicon does not wet or react with boron nitride during short-term exposure. Simplification and lower cost of fabricating the silicon containment vessels is believed possible based on this non-wetting property together with the high surface

tension of silicon. These two properties should prevent silicon from penetrating tight fitting mechanical joints, allowing the containment vessels to be fabricated from flat plates of boron nitride Long-term experimentation is necessary to verify this.

Most of the literature on molten silicon resulted from work in connection with semi-conductor fabrication and lacks data on long-term effects. This data is vital for successful design of a silicon based solar energy buffer receiver storage core.

Future work on the design of the HEDL high temperature receiver concepts should include tests on material compatibility at high temperatures, verification of the high temperature properties stated in the literature, and complete computer analysis. Projections of performance under different operating conditions will be expedited by development of a suitable computer model based on algorithms simulating performance of the individual components. HEDL recommends engineering tests be performed on each component prior to constructing the complete device. This will help save time by minimizing problems in the complete prototype.

APPENDIX

DETAILED DESIGN PERFORMANCE COMPUTATIONS

A. RADIANT ENERGY INPUT TO WINDOWS

Consider the peak solar flux entering annular ring-shaped regions of the outer window of the receiver. The following table summarizes the flux distribution:

Radius Region	Transmitted Flux*	Annular Area	Approximate Flux·Area
0 - 0.5 cm	1450 W/cm^2	0.79 cm^2	1.14 kW
0.5 - 1	1380	2.36	2.7
1 - 1.5	1300	3.93	4.1
2 to 3	1000	15.7	12.6
3 to 4	700	22.0	12.3
4 to 5	400	28.3	9.0
5 to 8	150	143.0	17.2
		TOTAL	64.4 kW†

Now, consider the total radiant input to the Al_2O_3 window. Ignoring losses in windows, and assuming perfect focus at the Al_2O_3 window for a 4.0 cm (1.6 inch) radius Al_2O_3 window, the radiant input to the Al_2O_3 window is:

$$P_{in} = 38.2 \text{ kW}$$

Power re-radiated from an 1800°C blackbody of the same area as the Al_2O_3 window is:

$$P_{out} = \underline{Al_2O_3 \text{ Window Loss}}$$

$$\text{Area} * \text{Radiance} = 50.3 \text{ cm}^2 \times 100 \text{ W/cm}^2 = 5030 \text{ watt} = 5.0 \text{ kW}$$

This is conservative, since the 5.0 kW value assumes loss into 0°K space. Actually, some of the angle into which the Al_2O_3 window radiates is occupied by the hot interior of the structure surrounding the quartz window.

---

* Transmitted flux is from curve of flux versus radial distance on page 5 of Sanders December 1979 report.

† The total flux·area adds up to slightly more than the actual power input since individual values were obtained graphically and are therefore approximate.

In addition, the greenhouse effect, which would tend to reduce losses through both the Al_2O_3 and quartz window, is ignored. However, the reflection and transmission losses of the windows are also ignored which partially compensates for ignoring the greenhouse effect.

B. RADIAL TEMPERATURE DROP THROUGH A CYLINDRIVAL GRAPHITE HEAT STORAGE CORE

Assume the initial temperature throughout a graphite cylinder of radius $0 < r \leq a$ at time $t = 0$ to be a uniform value $T = T_0$. Then, for a sudden onset of cooling at a constant rate at the surface, $r = a$, the temperature distribution can be adapted from the literature as[63]

$$T = T_0 - \left\{ \frac{2F_0\alpha t}{Ka} + \frac{F_0 a}{K}\left[\frac{r^2}{2a^2} - \frac{1}{4} - 2\sum_{n=1}^{\infty} e^{-\alpha_n^2 t/a^2} \frac{J_0(r\alpha_n/a)}{\alpha_n^2 J_0(\alpha_n)}\right]\right\} \quad (1)$$

where $\alpha = K/Cp$, K is thermal conductivity, C is the specific heat, ρ is the density, F_0 is the heat flux density at the cylinder's surface and α_n are the roots of $J_1(\xi) = 0$.

For graphite at 1200 to 1800°C,

$$C = 0.5 \frac{cal}{g°C}$$

$$K = 0.125 \frac{cal}{cm°C\ sec}$$

$$\rho = 1.7 \frac{g}{cm^3}$$

$$\alpha = 0.147 \frac{cm^2}{sec}$$

The average rate of power output from the graphite cylinder can be obtained as follows:

$\dot{m}$ = Mass flow rate of the working fluid (air).
C = Average specific heat of the working fluid.
Q_T = Total thermal power output
ΔT = Temperature increase of the working fluid as it passes through heat exchangers

With a fully charged storage core, the outlet gas temperature design point is 1370°C. When the core is reaching the end of its discharge cycle, the outlet gas temperature design point is 1170°C. The output power of the core is defined to be 60 kW for a gas outlet temperature 1370°C. The inlet gas temperature is defined to be 950°C in all cases. Since the gas flow is defined to be constant, the power output at the lower gas outlet temperature design point is lower. Mass flow, temperature and power are related by

$$\dot{m} = \frac{Q_T}{C\ \Delta T} .$$

The values of parameters at the upper and lower design points can be summarized as

Air Outlet Temperature	Air Inlet Temperature	Mass Flow Rate	Average Air Temperature	Air Average C	Thermal Power Output
1370°C	950°C	130 g/sec	1160°C	0.2625	60 kW
1170°C	950°C	130 g/sec	1060°C	0.2589	31 kW

Hence, the <u>average</u> power output during the discharge cycle is (60 + 31)/2 = 45.5 kW. As an expedient in these conceptual computations, the radial temperature drop through the graphite core was calculated using the average power rate. Refined design computations using a digital computer will use the complete power flow history during the discharge cycle in the radial temperature drop computation.

Assume the storage core is a graphite cylinder having a 20.32 cm (8-inch) diameter and 229 cm (90-inch) length. Desntiy of the core is assumed to be 1.7 gm/cm^3.

Weight of core = 126.5 Kg (278 lb)
Surface area of core = 1.462×10^4 cm^2
F_0 = Average heat flux at core surface = $0.7 \frac{cal}{cm^2 \ sec}$
a = radius of core = 10.16 cm

The term in brackets in equation (1) is given by a set of curves in reference (63) as a function of $\alpha t/a^2$. For this case, at r = a = 10.16 cm and t = 30 minutes,

$$\alpha t/a^2 = 2.56$$

The resulting term in the brackets is [ ] = 0.24.

Hence, the temperature at the outer surface of the cylinder after 30 minutes is

$$T_s = T_0 - F_0 \{416.7 + 81.3 [0.24]\}$$
$$= T_0 - 0.7 [436.2]$$
$$= T_0 - 305.3$$

Now since T_0 = 1800°C, the core surface temperature at the end of the 30 minute discharge cycle is T_s = 1494.7°C.

C. TEMPERATURE DROP THROUGH CORE-TO-CONTAINER GAP

Assume: 60 kW power total (4.10 $Watt/cm^2$ core surface flux) at high design point.
31 kW power total (2.12 $Watt/cm^2$ core surface flux) at low design point.
Surface area of core = 14619 cm^2 (20.32 cm dia. x 229 cm long)
ε = 1.0 for wall and core

Core surface temperature = T_1 = 1800°C (beginning of discharge)
or 1494°C (end of discharge)

Core enclosure wall temperature = T_2 = 1455°C (beginning of discharge)
or 1207°C (end of discharge)

Then,

$$P_o = \sigma\varepsilon(T_1^4 - T_2^4)$$

where σ is the Stefan-Boltman constant, and ε is emissivity, P_o is power, assuming $\varepsilon \sim 1$.

$$T_2^4 = T_1^4 - \frac{P_o}{\sigma\varepsilon} .$$

The Stefan-Boltzman constant is 5.6686×10^{-12} Watt cm^{-2} deg^{-4} sec^{-1}, so using the information given above, at the beginning of discharge (60 kW)

$$T_2 = 2052°K = 1779°C$$

Hence, a core-to-container temperature drop of only (1800 - 1779) = 21°C would be necessary to sustain the 60 kW energy flow needed. The movable insulating shield would thus be nearly closed at this time since the enclosure wall temperature for 60 kW transfer to the working gas is only 1455°C (see Figure 5). At 31 kW (end of discharge) with an outer core surface temperature of 1494°C the corresponding enclosure wall temperature would be 1477°C for a drop through the gap of only 17°C. Hence, even at the low design discharge point, the shield would remain partially closed since the enclosure wall temperature required for 31 kW transfer to the gas is only 1207°C.

D. HEAT FLOW THROUGH THE FIBER FORM INSULATOR SHIELD AROUND CORE

The movable insulation shield was assumed to be a fiber-form insulating cylinder having inner and outer radii, a and b, respectively, a thermal conductivity of 8.6×10^{-4} cal/sec-cm-°C, an inside temperature of 1800°C and an

outside temperature of 1425°C was assumed. All heat flow was considered to be radially outward, with no flow through the ends. Hence, the heat flow is described by

$$Q = \frac{2\pi K\ell(T_{inside} - T_{outside})}{\ln(b/a)} \qquad (2)$$

where ℓ is the length of the cylinder assumed to be 229 cm.

Hence,

$$Q = \frac{463.2}{\ln(b/a)} \frac{cal}{sec} = \frac{1.94}{\ln(b/a)} kW.$$

The heat flow for several thicknesses of insulator shield are shown below. This heat is not lost, but is picked up by the gas as it flows through the heat exchanger outside the core enclosure. The inner radius, a, of the cylinder is assumed to always be 10.16 cm. Thickness changes cause only the outer radius, b, to change.

Outer Radius b (cm)	Thickness (cm)	$\frac{b}{a}$	$\ln(\frac{b}{a})$	Total Q (kW) for 20.3 cm I.D. x 229 cm long shield
12.70	2.54	1.25	0.22	8.8
15.24	5.08	1.50	0.41	4.7
17.78	7.62	1.75	0.56	3.5
35.56	25.4	2.50	0.92	2.1

E. TEMPERATURE DROP THROUGH THE SiC CORE ENCLOSURE WALL

Assume a total power flow of 60 kW distributed uniformly over the entire area of the core enclosure wall. This wall is a 1.27 cm (1/2-in) thick cylinder having a mean diameter of 29.2 cm (11 1/2-in), a length of about 229 cm (90 inch) and a total wall area of 2.097×10^4 cm^2. Heat flux flowing through the wall is therefore 0.684 cal/cm^2 sec. Since the thermal conductivity of SiC is 0.04 cal/cm-sec-°c at 1400°C[64], the temperature drop through the wall at 60 kW is

$$\Delta T = \frac{q\ell}{K} = 21.7°C$$

where q is the heat flux, ℓ is the wall thickness and K is the thermal conductivity of silicon carbide at 1400°C.

F. TEMPERATURE DROP RADIALLY OUTWARD THROUGH THE HEAT EXCHANGER

The heat exchanger is assumed to be a 5.08 cm (2-inch) thick cylinder that fits around the storage core. Longitudinal cooling gas passages 0.635 cm (1/4-inch) in diameter having 0.95 cm (3/8-in) between centers run the full length of the cylinder. There are five concentric layers of gas passages in the wall of the cylinder. The passages in successive layers are assumed to be lined up along radii of the cylinder. Hence, there are solid regions of material between the lined-up gas passages. These regions can be approximated as "fins" from which heat removal is accomplished via the gas passages. An equivalent coefficient of heat transfer for the "fins", corresponding to that for ordinary rectangular fins, can then be calculated to make use of a standard textbook solution for cooling fins. This temperature distribution can be used directly as an approximation of the radial distribution in the heat exchanger.

Radial temperature, referenced to the temperature of the cooling medium as zero can then be computed for a cylinder in which the wall thickness is much smaller than the diameter as[65]

$$V = V_0 \frac{\cosh\left[(L - X)\sqrt{2H/KD}\right]}{\cosh\left[(L\sqrt{2H/KD}\right]}$$

where V_0 is the inner surface temperature*, H is the coefficient of surface heat transfer, X is the radial distance outward from the inside surface, K is the thermal conductivity of the heat exchanger material, L is the radial thickness of the heat exchanger, and D is the equivalent thickness of fin conservatively estimated to be the 3 mm of material between holes. Figure 5

* This is the temperature at the core container/heat exchanger interface.

shows this information pictorially.

For a set of 585 tubular gas passages of diameter d = .635 cm and spaced on .95 cm (3/8") centers, the cross sectional area of a gas passage is

$$A_p = \frac{d^2}{2}\pi = \pi(0.32\ \text{cm})^2 = 0.317\ \text{cm}^2.$$

Using a specific heat for air at an outlet temperature of 1370°C (a mean temperature of 1160°C) of C = 0.26, then the mass flow for a 60 kW thermal power output is

$$\dot{m} = \frac{\text{Power output}}{C\ (1370°C - 950°C)} = 130\ \text{gm/sec}$$

through the heat exchanger or, dividing by the number of passages,

$$\dot{m}_p = .222\ \text{gm/sec}$$

through a given passage of the heat exchanger. Since the density ρ_A of air at 1160°C and 3 atmospheres pressure is

$$\rho_A = 7.512 \times 10^{-4}\ \text{gm cm}^{-3},$$

the volumetric flow through a given passage is

$$\dot{V}_p = 296\ \text{cm}^3\ \text{sec}^{-1}.$$

The velocity (average) is then

$$U_A = \frac{\dot{V}_A}{A_p} = 935\ \text{cm sec}^{-1}$$

The heat transfer coefficient H_p for gas passages may be determined as follows:

The Reynolds number

$$N = \frac{U_A d \rho}{\mu} = \frac{Gd}{\mu},$$

where the mass velocity

$$G = 0.70 \text{ gm sec}^{-1} \text{ cm}^{-2}$$

and μ is viscosity of the air in the gas passages (5.32×10^{-4} poise).

Then,

$$N = \frac{Gd}{\mu} = 836,$$

which clearly implies laminar flow.

It has been found that the coefficient of heat transfer for a circular tube with laminar flow can easily be computed[66] when

$$\frac{\dot{m}_p C}{K_A \ell} < 2.$$

where K_A is the thermal conductivity of the gas and ℓ is the length of the gas passage. In this case, the gas is uniformly heated through the entire cross section of the passage to the temperature of the tube wall.

For the case under consideration,

$\dot{m}_p = 0.222 \text{ gm sec}^{-1}$, $C = 0.2625 \text{ cal gm}^{-1}{}^\circ\text{C}^{-1}$, and

$K_A = 2.17 \times 10^{-4} \text{ cal cm}^{-1} \text{ sec}^{-1}{}^\circ\text{C}^{-1}$.

The gas temperature across the passage is then equal to the wall temperature when

$$\frac{\dot{m}_p C}{Ka\ell} = \frac{267}{\ell} < 2.$$

which requires, in this case,

$$\ell > 133 \text{ cm.}$$

For a graphite storage core of 130 Kg mass and 20.3 cm diameter, if the density of the graphite is

$$\rho = 1.75 \text{ gm cm}^{-3},$$

then the core volume is

$$V_G = 7.43 \times 10^4 \text{ cm}^3.$$

The core length can be found from

$$\ell = \frac{V_G}{\pi r^2},$$

where r is the radius of the graphite core. This yields

$$\ell = 229 \text{ cm},$$

satisfying the condition requiring $\ell > 133$ cm.

Using this value for the length of the gas passages, the heat transfer coefficient for the passages[66] is

$$H_p = \frac{2\dot{m}C}{\pi d\ell} = 2.53 \times 10^{-4} \text{ cal cm}^{-2} \text{ sec}^{-1} {}^\circ\text{C}^{-1}$$

An equivalent flat-plate "fin" surface coefficient, H_F, can be calculated where

$$H_F = H_p \frac{\text{Internal surface area of 10 passages adjacent to a fin}}{2 \text{ (area of two sides of fin)}}$$

The 585 tubular gas passages are placed in 117 rows of five passages spaced evenly around the cylindrical heat exchanger, each row lined up along a radius. Each equivalent "fin" is then bordered by 10 passages. The internal surface area of the passages is then

$$10A_{SA} = 10\pi d\ell = 4568 \text{ cm}^2.$$

The double sided surface area of a "fin" 5.08 cm by 229 cm is 2327 cm^2, hence

$$H_F = 0.98\ H_p = 2.41 \times 10^{-4} \text{ cal cm}^{-2} \text{ sec}^{-1} {}^\circ\text{C}^{-1}.$$

Since the mean thermal conductivity over the temperature range of interest of the heat exchanger material, silicon carbide, is approximately

$$K = 5 \times 10^{-2} \text{ cal sec}^{-1} \text{ cm}^{-1} {}^\circ\text{C}^{-1},$$

then

$$\sqrt{2H_F/KD} = 0.179 \text{ cm}^{-1}$$

and the temperature at the outer periphery of the heat exchanger is

$$V_L = V_0 \frac{\cosh [0]}{\cosh [(0.179 \text{ cm}^{-1})\ 5.08 \text{ cm}]} = V_0 \frac{1}{\cosh [0.911]}$$

or

$$V_L = 0.69\ V_0.$$

The total heat transferred from the "fin" is

$$Q = \int_0^L H_F V_0 \frac{\cosh [(L - X)\sqrt{2HF/KD}]}{\cosh [L\sqrt{2HK/KD}]} dX = \frac{2H_F V_0}{\sqrt{2HF/KD}} \tanh L\sqrt{2HF/KD}$$

or

$$Q = V_0 \sqrt{2HF/KD} \tanh L \quad 2HF/KD = 1.96 \times 10^{-3} V_0 \text{ cal cm}^{-1} \text{ sec}^{-1} {}^\circ\text{C}^{-1}$$

where V_0 is the core container temperature in °C.

The total Q_T can then be calculated by

$$Q_T = Q^* \text{ (number of "fins") x (length of "fins")}$$
$$= (1.96 \times 10^{-3} \text{ cal cm}^{-1} \text{ sec}^{-1} {}^\circ\text{C}^{-1})(117)(229 \text{ cm}) V_0$$
$$= 52.5 \text{ cal sec}^{-1} {}^\circ\text{C}^{-1} V_0$$
$$= (220 \text{ W} {}^\circ\text{C}^{-1}) V_0.$$

Since Q_T is required to be 60 kW,

$$V_0 = \frac{Q_T {}^\circ\text{C}}{220 \text{ W}} = 273^\circ\text{C}.$$

Recall that V_0 is the temperature at the interface between the heat exchanger and the core enclosure referenced to a gas temperature of zero degrees. Since the actual average gas temperature is 1160°C, the temperature of the inner wall of the heat exchanger, which is assumed to be the same as the temperature of the outer wall of the core container, is

$$V_{\text{core container}} = 273 + 1160 = 1433^\circ\text{C}$$

and the temperature at the outer periphery of the heat exchanger is

$$V_L = 0.69 V_0 = 188^\circ\text{C}$$

above the average gas temperature, or

$$V_{\text{periphery}} = 188^\circ\text{C} + 1160^\circ\text{C} = 1348^\circ\text{C}.$$

The radial temperature drop across the heat exchanger is

$$\Delta V = 85°C.$$

These temperatures apply only for the case where the outlet temperature of the gas is 1370°C with an inlet temperature of 950°C and power output from the core of 60 kW at the beginning of a discharge cycle.

Temperatures in the heat exchanger wall at the <u>end</u> of a discharge cycle can be similarly computed as follows:

$\dot{m}$ = 130 gm/sec (defined total)
$\dot{m}_p$ = 0.22 gm/sec (single passage)
$\rho_A = 8.06 \times 10^{-4}$ gm cm^{-3} (at 1060°C).

Then volumetric flow through a single passage is

$$\dot{V}_A = 275 \text{ cm}^3 \text{ sec}^{-1}.$$

The velocity average is then

$$U_A = \frac{\dot{V}_A}{A_p} = 855 \text{ cm sec}^{-1}.$$

The Reynolds number for this case is not much different than that calculated above for the conditions at the start of discharge, since the only changed parameter is the viscosity of air. The viscosity at 1060°C is approximately 4.91×10^{-4} poise, and the thermal conductivity is $K = 2.3 \times 10^{-4}$. Hence, the flow at the end of discharge is still laminar. The parameter group $\dot{m}_p C / K_A \ell$ is then

$$\frac{\dot{m}_p C}{K_A \ell} = 1.11.$$

Thus, the requirement that the parameter group be less than 2 is still met, with

$$H_p = \frac{2\dot{m}_p C}{\pi d \ell} = 2.56 \times 10^{-4} \frac{\text{cal}}{\text{cm}^2 \text{ sec } °C}$$

and, as above,

$$H_F = 0.98\ H_p = 2.51 \times 10^{-4}\ \frac{cal}{cm^2\ sec°C}.$$

The mean thermal conductivity of SiC given above can be used with the other parameters to obtain the value of the arguments for the hyperbolic functions in the first equation in this section. Hence,

$$\sqrt{2HF/KD} = 0.178\ cm^{-1}$$

and the outside surface temperature of the heat exchanger is

$$V_L = V_0 \frac{\cosh [0]}{\cosh [0.178\ (5.08)]} = 0.70\ V_0.$$

As before, the total heat transfer from a fin is

$$Q_T = V_0 \sqrt{2H_F KD}\ \tanh L \sqrt{2H_F/KD}$$
$$= 2.03 \times 10^{-3}\ V_0\ cal\ cm^{-1}\ sec^{-1}°C^{-1}.$$

The total thermal power flow from the "fins" is

$$Q_T = Q \times (\#\ "fins") \times (length\ of\ "fins")$$
$$= 54.4\ V_0\ cal\ sec^{-1}°C^{-1}$$
$$= 226\ V_0\ W\ °C^{-1}.$$

At the minimum power design point, when Q_T is 31 kW, we can thus obtain

$$V_0 = \frac{Q_T\ (Watts)}{227} = \frac{3.1 \times 10^4}{227} = 136°C.$$

As before, we must add the actual average gas temperature to this to get the temperature at the intersection between the core containment and the heat exchanger. Hence, for 31 kW minimum power design point,

$$V_{core\ container} = 136 + 1060 = 1196°C.$$

The outer peripheral temperature of the heat exchanger is then

$$V_L = 0.70\ V_0 = 96°C$$

referenced to zero gas temperature. Adjusting V_L for the true gas temperature, we obtain

$$V_{periphery} = 95 + 1060 = 1155°C$$

at the minimum power design point at the end of discharge. The temperature drop across the heat exchanger's 5.08 cm thickness is

$$\Delta V = 1196 - 1155 = 41°C$$

at the end of discharge.

All of the above computations assumed that discharge occurs slowly enough that the temperature values are essentially steady state.

G. GAS PRESSURE DROP DUE TO FLOW THROUGH HEAT EXCHANGER

The heat exchanger is a cylinder having an I.D. of 30.5 cm (12 inches) and an O.D. of 35.6 cm (14 inches). These are 585 gas passages (0.635 cm) (1/4 inch) in diameter running longitudinally through the full length of the cylinder wall (229 cm). Characteristics of the heat exchanger are listed below:

SiC Heat Exchanger Pneumatic Values

Gas (Air) Flow Design Point = 130 gm/sec at 1060°C to 1160°C average gas temperature and 45 psia outlet pressure.

Density of Gas (Air) at 1160°C, 45 psia = 7.5×10^{-4} gm/cm^3.

Total number of 0.635 cm (1/4 inch) diameter passages = 585.

Velocity of Air in Passages = 935 cm/sec at 1160°C and 45 psia.

Specific heat of 1160°C, 45 psia air = 0.26 $\frac{cal}{gm°C}$.

Viscosity of air at 1160°C = 5.32×10^{-4} poise.

The Reynolds number equation appropriate for the present case is[67]

$$N = \frac{vd\rho}{\mu} = 837.0$$

Where d = gas passage diameter
v = velocity
ρ = density
γ = specific weight = ρg
μ = viscosity of gas

Hence, gas flow through the heat exchanger is laminar.

The pressure drop for 1170°C, 45 psi air flowing through the gas passages is given by[68]

$$P = \frac{f\ell v^2 \gamma}{2dg} = 1.18 \times 10^5 f \frac{dynes}{cm^2}$$

where f is the friction factor, ℓ is the length of the passages (cm) and g is the acceleration of gravity (980.65 cm/sec^2). The friction factor is[68]

$$f = \frac{64}{N} = 0.0765.$$

Hence, we obtain the pressure drop as

$$P = 9.04 \times 10^3 \frac{dynes}{cm^2} = 0.130\ lb/in^2.$$

which is insigificant. Due to the low magnitude of this pressure drop, additional pressure drops that would occur due to the ends of the gas passages were not computed.

REFERENCES

1. G. S. Brady and H. R. Clauser, Materials Handbook, 11th ed. (San Francisco: McGraw-Hill, 1977), p. 356.

2. E. N. Marmer, O. S. Gurvich, and L. F. Mal'tseva, High Temperature Materials, (Holon, Israel: Freund Publishing House, 1971), p. 168.

3. Ibid, p. 144

4. Ibid, P. 147.

5. Brady, op. cit., p. 356.

6. Thermophysical Properties Research Center at Purdue University, Thermophysical Properties of High Temperature Solid Materials, vol. 1, Y. S. Touloukian, ed. (New York: MacMillan, 1967), p. 118.

7. Marmer, op. cit., p. 134.

8. Touloukian (1967), op. cit., p. 110 ff.

9. Marmer, op. cit., p. 140.

10. Brady, op. cit., p. 105.

11. P.T.B. Shaffer, Materials Index (New York: Plenum Press, 1964), p. 266.

12. Ibid.

13. Touloukian (1967), op. cit., vol. 5, p. 499.

14. Ibid, p. 503.

15. Ibid, p. 505.

16. Y. S. Touloukian and D. P. DeWitt, Thermophysical Properties of Matter, vol. 8 - Thermal Radiative Properties Nonmetallic Solids, (New York: IFI/Plenum Data Corp., 1972), p. 1037.

17. Touloukian (1967), op. cit, vol. 5, p. 507.

18. Brady, op. cit., p. 104.

19. Shaffer, op. cit., p. 81.

20. Ibid.

21. Touloukian (1967), op. cit., vol. 5, p. 25.

22. Ibid, p. 27.

23. Ibid, p. 29.

24. Touloukian, (1972), op. cit., p. 851.

25. Touloukian (1967), op. cit., vol. 5, p. 33.

26. Brady, op. cit., p. 700.

27. R. F. Adamsky, Journal of Physics and Chemistry, vol. 63 (1959), p. 305.

28. J. A. Cornie, "Characterization, Shaping, and Joining of SiC/Superalloy Sheet for Exhaust System Components", (NASA-CR-135301, July 20, 1977), p. 19.

29. Shaffer, op. cit., p. 108.

30. C. J. Smithells, Metals Reference Book, 4th ed., vol. 3 (New York: Plenum Press, 1967), p. 1016.

31. Touloukian (1967), op. cit., vol. 5, p. 123.

32. Ibid, p. 125.

33. Touloukian, op. cit., p. 793.

34. Touloukian, op. cit., p. 129.

35. Shaffer, op. cit., p. 308.

36. Marmer, op. cit., p. 84.

37. Shaffer, op. cit., p. 311.

38. Ibid, p. 312.

39. Touloukian (1967), op. cit., vol. 4, part 1, p. 41.

40. Ibid, p. 8.

41. Ibid, p. 11.

42. Touloukian (1972), op. cit., p. 179.

43. Touloukian (1967), op. cit., vol. 4, part 1, p. 47.

44. Brady, op. cit., p. 344.

45. Sanders Associates, Inc., "High Temperature Solar Thermal Receiver", (Final Report for J. P. L. Contract No. 944545, December 1979), p. 75.

46. Ibid.

47. Touloukian (1967), op. cit., vol. 4, part 1, p. 353.

48. Sanders, op. cit., p. 39.

49. Touloukian (1967), op. cit., vol. 4, part 1, p. 361.

50. Touloukian (1972), op. cit., p. 403.

51. Touloukian (1967), op. cit., vol. 4, part 1, p. 367.

52. Johns-Manville Refractory Products, "Cera Form Special Shapes", (Data Sheet IND-35, August 1980).

53. Ibid.

54. Ibid.

55. "Fiber Form Insulation Data Package," Submitted by: Fiber Materials, Inc., Biddeford Industrial Park, Biddeford, Maine, 04005.

56. Marmer, op. cit., p. 168.

57. Fiber Form, op. cit.

58. Ibid.

59. Touloukian, op. cit., p. 118.

60. Fiber Form, op. cit.

61. Ibid.

62. From private conversation with Lou Lander of Fiber Materials, Inc.

63. H. S. Carslaw and J. C. Jaeger, "Conduction of Heat in Solid", p. 203, 2nd ed., Oxford, 1959.

64. Ibid, p. 189.

65. Ibid, p. 141.

66. W. H. McAdams, Heat Transmission, pp. 230-232, McGraw-Hill (1954).

67. V. L. Streeter, Fluid Mechanics, pp. 108-210, McGraw-Hill, 1951.

68. Ibid.

DISTRIBUTION

JPL (26)

R. Manvi (25)
J. Walsh

DOE/RL

M. Plahuta

FTFF/PO

H. Ranson

HEDL (52)

S. W. Berglin	W/A21	(5)
M. B. Boone	W/A21	
R. W. Davis	W/E19	(10)
D. R. Green	W/A56	(10)
I. F. Marshall	W/C125	(2)
M. P. Nolan	W/D26	(2)
L. S. Price	W/A56	(10)
E. M. Sheen	W/A56	(5)
J. M. Yatabe	W/C22	
Central Files	W/C110	(5)
Publication Services	W/C112	(2)